arXiv:1212.1705v1 [cond-mat.supr-con] 7 Dec 2012

On the intermediate superconducting state in a flat slab

V. Kozhevnikov[1], R. J. Wijngaarden[2], J. de Wit[2] and C. Van Haesendonck[3]
[1] *Tulsa Community College, Tulsa, Oklahoma 74119, USA*
[2] *VU Amsterdam, 1081 HV Amsterdam, The Netherlands*
[3] *Laboratory of Solid-State Physics and Magnetism, KU Leuven, BE-3000 Leuven, Belgium*

The intermediate state (IS) in a very clean film of a Pippard superconductor (In with mean free path 11 μm) was investigated using simultaneous magneto-optical imaging and electrical transport measurements. A consistent framework for the IS in a flat slab is presented for the first time.

PACS numbers:

The rich physics of the intermediate state (IS) in type-I superconductors and unsolved fundamental problems continue to keep the IS in a focus of interests of superconductivity [1, 2]. Two of those problems are the magnetic flux density B in the normal (N) domains and the critical field H_{ci} for the IS-N transition. On the other hand, the IS provides access to one of the most fundamental parameters, i.e. the Pippard coherence length ξ_0 (size of Cooper pairs), however an experimentally verified recipe to extract ξ_0 from the IS parameters is still missing. Similar problems, i.e. B in vortex cores, or size of the cores, and extraction of microscopic parameters from parameters of the mixed state (MS), are among central problems of unconventional superconductivity [3]. Due to an ultimate relationship between the IS and the MS [4], one can expect that solution of the problems for the former will help to solve them for the latter.

Ever since Landau introduced a laminar model (LLM) for a slab in a transverse field [5], many theoretical models of the IS have been proposed, however no one of those is adequate. Here we report on an experimental study of the IS resulting in the development of a new model for the slab in an arbitrary oriented magnetic field. The model, based on Tinkham's interpretation of the LLM [6], is surprisingly simple. Nevertheless it correctly accounts for the main properties of the IS including ξ_0.

When a type-I superconductor with demagnetizing factor η [6] is subjected to a weak magnetic field H, the sample is in the Meissner state until H reaches $H_i \equiv (1-\eta)H_c$, H_c being the thermodynamic critical field. At H_i the sample undergoes a transition to the IS, where it brakes up into N and superconducting (S) domains with flux densities B and zero, respectively. Under increasing H the normal fraction $\rho_n \equiv V_n/V$ (V_n and V are the volumes of N domains and of the sample, respectively) increases until the entire sample becomes normal at H_{ci}. Usually one assumes that H_{ci} is equal to [7] or slightly less than [8] H_c. Below it is shown that this is true only for very thick samples.

The shape of the IS domains depends on a big variety of factors (sample geometry, material, purity, *etc*) and is unpredictable due to small energy difference for different domain shapes [9]. However, the shape is simple in two cases: a long cylinder in the transverse field and a flat slab in a strongly slanted field. In the former η=0.5 and domains are discs perpendicular to the sample axis. In the latter η=1 (H_i=0) and domains are linear laminae [4]. IS in the flat slab can be investigated using magneto-optics (MO) [9]; this is an experiment we performed.

Primarily we focus on the following questions. (1) How does the flux density B and the critical field H_{ci} depend on parameters of material, and how do these quantities evolve with magnitude and orientation of H? (2) How can the domain-wall energy parameter δ (and therefore also the Ginzburg-Landau (GL) $\xi(T)$ and the Pippard ξ_0 coherence lengths) be inferred from the laminar structure? Relationship between δ, $\xi(T)$ and ξ_0 depends on material and its purity. For Pippard superconductors (materials with the GL parameter $\kappa \ll 1$) in the pure limit (the elastic mean free path $\ell \gg \xi_0$) $\delta(T) = 1.89\xi(T) = 1.40\xi_0/(1-t)^{0.5}$, where $t = T/T_c$ [6].

On the first glance the answers are available in classic texts [4, 6–8]. However it turns out that ξ_0 in In, directly determined from combined Low-Energy Muon Spin Rotation (LE-μSR) and Polarized Neutron Reflectometry (PNR) experiments (380 nm) [10], differs from that following from δ obtained from the IS (240 nm) [11]. This signals for inadequacy of theoretical models used for interpretation either of the LE-μSR/PNR data or of the IS data. This discrepancy is even more intriguing if one takes into account that the IS studies [11, 12] "played an important role in establishing the GL theory in the first place" [6]. To resolve this contradiction was an original motivation for this work.

The IS structure in the flat slab was first treated by Landau in 1937 [5]. In this work Landau established the concept of a surface tension of a S/N interface γ (δ was later defined as $8\pi\gamma/H_c^2$ [13]) and proposed the LLM. Assuming that $B = H_c$, Landau calculated the shape of rounded corners of a cross section of the S-laminae. The rounded corners yield an excess energy of the system competing with the S/N interface energy. Minimizing a sum of these two energy contributions, Landau obtained the period of the laminar structure $D = \sqrt{\delta d/f_L(\rho_n)}$, where d is the sample thickness and $f_L(\rho_n)$ is a spacing function with $\rho_n = h \equiv H/H_c$ [7].

Soon thereafter Landau, advised by Peierls, admitted that LLM is unstable because roundness of the corners makes B near the surface less than H_c. Landau then introduced a "branching" model [13], which was shown to be inadequate by Meshkovsky and Shalnikov in 1947. Due to that in 1951 Lifshitz and Sharvin returned back to LLM and calculated numerically $f_L(\rho_n)$ and B; identical results have later been obtained analytically by Fortini and Paumier [7]. B in LLM, being H_c in the bulk, near the surface is $0.66H_c$ at low H and increases with H up to H_c at the IS-N transition. 50 years later direct bulk μSR measurements of B in a Sn slab in a transverse field revealed that $B(H)$ starts from H_c and decreases with H down to H_{ci} [14]. Such a dependence for $B(H)$ had been anticipated by Tinkham [6].

De Gennes [8] noticed that a positive γ should reduce H_{ci}. Assuming a small reduction, De Gennes obtained for the transverse configuration $H_{ci\perp} = H_c[1 - 0.9(\delta/d)^{0.5}]$.

Tinkham [6] modified LLM in a different way. He noticed that the dominant contribution to the excess energy term comes from inhomogeneity of the field outside the sample near its surface and therefore contribution due to rounded corners can be neglected. Tinkham computed this energy introducing a "healing length" L_{heal} over which the field relaxes to its uniform state away from the sample: $L_{heal}^{-1} = D_n^{-1} + D_s^{-1}$, where D_n and D_s are the width of the S- and N-laminae, respectively. For the same reason Tinkham assumed a rectangular cross section of the laminae and hence a uniform B, which was allowed to be $\leq H_c$. Tinkham's expression for D has a form similar to that in LLM with $f_L(\rho_n)$ substituted by $\rho_n^2(1-\rho_n)^2$. For H_{ci} Tinkham obtained

$$H_{ci\perp} = H_c[(1 + 4\delta/d)^{0.5} - 2(\delta/d)^{0.5}] \tag{1}$$

with no preliminary restrictions for the H_{ci} reduction.

The structure expected from the LLM has *never* been observed. Images, reported from the 1950s on revealed far more complicated flux patterns than that in the LLM and that domains are often corrugated laminae [9]. Balashova and Sharvin in 1956 and Faber [15] proposed that the corrugations stabilize the laminar structure. However the disordered laminae in the perpendicular field might imply that asymmetry in the field configuration is able to change the structure in favor of the Landau's prediction, as was first predicted by Dzyaloshinskii in 1955 [16].

Sharvin [12] was the first to observe the ordered laminar pattern in a *strongly* tilted field on 50 mm × 2 mm (diameter × thickness) Sn [12] and In [11] samples. From the images, obtained utilizing a Bitter method [9], Sharvin measured D at different temperatures and calculated $\delta(T)$ using an extended LLM, which assumes $B_\parallel = H_\parallel$ ($B_\parallel$ and $H_\parallel$ are in-plane components of B and H, respectively) on top of Landau's original assumption that $B = H_c$. Sharvin's equation for D has a form

$$D^2 = \frac{\delta d}{f_L(\rho_n)} \cdot \frac{H_c^2}{H_c^2 - H_\parallel^2}. \tag{2}$$

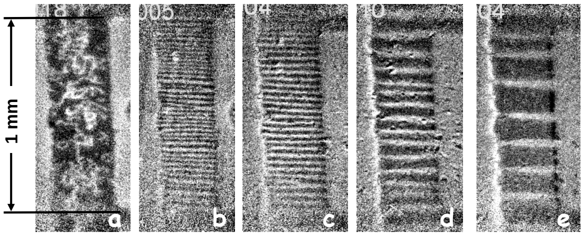

FIG. 1: MO images taken at 2.5 K. Superconducting regions are black. ($H_\parallel$ in Oe, $H_\perp$ in Oe): a, (0, 1); b, (60, 8); c, (100, 6); d, (110, 3); e, (115, 1.3).

The value of $\delta(0)$ obtained for In using Eq. (2) [11] is that from which we started our story. Faber [15] criticized Eq. (2) arguing that $H_\parallel$ may alter the shape of the laminae corners. One can add that if $B_\parallel = H_\parallel$ the magnetic flux is not conserved and therefore the energy balance in the system has to be reconsidered.

From what was said follows that validity of the extended LLM [12] is questionable. Therefore the value of ξ_0 following from $\delta(0)$ obtained in Ref. 11 is questionable as well. On the other side, the $\delta(T)$ dependence obtained by Sharvin is correct because it agrees with the GL theory. And on the third side, the question how to extract δ from the IS pattern in the tilted field remains to be answered. The last two issues along with the questions on B and H_{ci} are addressed below.

The MO imaging was achieved using a set-up equipped with a 3D vector magnet. The sample was a 2.5 μm thick In film deposited on a SiO$_2$ wafer. The film residual resistivity ratio was 540, and the elastic mean free path $\ell \approx 11\,\mu$m. The rest film characteristics were the same as those reported in Ref. 10. Overall, the film was a Pippard superconductor ($\kappa \simeq 0.07$) in the pure limit. The sample length was 1 mm and the ratio width/thickness was 120, meaning that for the transverse and longitudinal fields η is 1 and 0, respectively. Images were taken simultaneously with measurements of the electrical resistance R using a small low frequency (11 Hz) AC current.

Typical images are presented in Fig. 1. Contrary to Pb [2], no flux tubes were observed in our In sample both for increasing and decreasing $H_\perp$. At $H_\perp \lesssim 1$ Oe fractionated laminae were seen in some runs. In the transverse field the pattern was *disordered laminae* (Fig. 1a) independent of the history of the applied field. This suggests that the laminar structure is a ground state topology of the IS. The same conclusion was drawn for Al [15]. Difference in the pattern in Pb from the pattern in In and Al can be attributed to a large difference in κ (0.6 for Pb and 0.01 for Al) and, accordingly, in γ for these metals: γ in Pb is much smaller than that in Al and In [9].

While D_n (D_s) increased (decreased) and R varied linearly with $H_\perp$, the period $D = D_n + D_s$, being depended on $H_\parallel$, was constant at $0.3 \lesssim H_\perp/H_{ic\perp} \lesssim 0.8$. Near $H_\perp = 0$ and $H_{ci\perp}$ number of the laminae $\aleph$ decreases. The IS-N transition at decreasing field was accompanied by supercooling of the N-state. This confirms that the IS-N transition is a first order phase transition [4].

Fig. 2 presents the sample phase diagram $H_c(T) = H_{c\parallel}(T)$ measured with a DC magnetometer. It is compared with data we measured on other samples and with data from Ref. 17. The $H_c(T)$ curve was used for *in situ* determination of the sample temperature. The lower curve presents $H_{ci\perp}(T)$ at $H_\parallel = 0$, determined on disappearance of the last S-lamina in MO images and from $R(H_\perp)$ measurements; the two perfectly coincide. The stars represent $H_{ci\perp}$ calculated from Eq. (1) with $\xi_0 = 380\,\mathrm{nm}$ and are clearly consisted with the experimental data. De Gennes' formula yields values of $H_{ci\perp}$ considerably exceeding the experimental data. Hence Tinkham's interpretation of the LLM is used for further analysis.

The model. Since we adopt Tinkham's approach and *in agreement with the experimental images*, the N- and S-domains are assumed to be rectangular parallelepipeds extending in the $H_\parallel$ direction. The contribution of the negative surface tension at the S/vacuum interface is neglected since the penetration depth $\lambda \ll d$. The out-of-plane and in-plane demagnetizing factors are $\eta_\perp$=1 and $\eta_\parallel$=0, respectively. The former means that $B_\perp \rho_n = H_\perp$ (conservation of the flux of the out-of-plane component of the magnetic field), whereas the latter means that $B_\parallel = H_\parallel$ and therefore the flux of $B_\parallel$ is not conserved. Hence an appropriate thermodynamic potential is $\tilde{F} = F - V(B_\parallel H_\parallel/4\pi) = F - V_n(H_\parallel^2/4\pi)$, where F is free energy [7]. Summing up the sample free energy at zero field, energy of the field B in the sample, energy of S/N interfaces and the excess energy of the field over the healing length, one obtains for $\tilde{f} = \tilde{F}/V$:

$$\tilde{f} = f_{n0} - (1-\rho_n)\frac{H_c^2}{8\pi} + \frac{H_\perp^2}{8\pi\rho_n} - \rho_n\frac{H_\parallel^2}{8\pi} + 2\frac{H_c^2}{8\pi}\frac{\delta}{D} + 2\frac{H_\perp^2}{8\pi}\frac{D}{d}(1-\rho_n)^2, \quad (3)$$

where f_{n0} is the free energy density of the sample in the normal state at zero field.

Similar to the case of the LLM, competition between the last two terms provides the equilibrium D:

$$D^2 = \frac{d\delta}{\rho_n^2(1-\rho_n)^2}\frac{H_c^2}{B_\perp^2} = \frac{d\delta}{(1-\rho_n)^2}\frac{H_c^2}{H_\perp^2}. \quad (4)$$

Substituting (4) in (3) one obtains

$$\tilde{f} = f_{n0} + \frac{H_c^2}{8\pi}[\rho_n - 1 + \frac{h_\perp^2}{\rho_n} - \rho_n h_\parallel^2 + 4h_\perp\sqrt{\frac{\delta}{d}}(1-\rho_n)], (5)$$

where $h_\perp = H_\perp/H_c$ and $h_\parallel = H_\parallel/H_c$.

Eq. (5) has a minimum yielding equilibrium ρ_n:

$$\rho_n^2 = h_\perp^2/(1 - 4h_\perp\sqrt{\delta/d} - h_\parallel^2). \quad (6)$$

At SI-N transition ρ_n=1, hence

$$h_{ci\perp} = \sqrt{4(\delta/d) + 1 - h_\parallel^2} - 2\sqrt{\delta/d}. \quad (7)$$

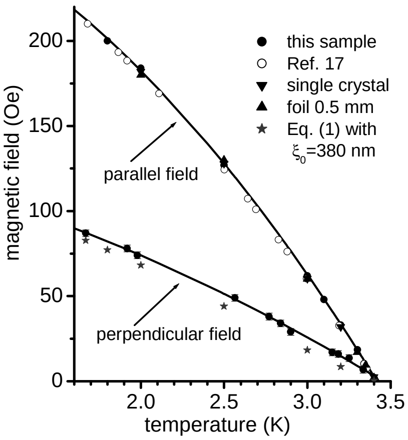

FIG. 2: The phase diagram of our sample in the parallel and perpendicular fields. The star symbols correspond to $H_{ci\perp}$ calculated from Eq. (1) using ξ_0=380 nm. The full curves are parabolic fits of the data obtained with our sample.

Finally, the reduced flux density $b = B/H_c$ is

$$b^2 = b_\perp^2 + b_\parallel^2 = 1 - 4h_\perp\sqrt{\delta/d}. \quad (8)$$

Obtained expressions satisfy limiting cases, i.e. $\rho_n \to 0$ at $H_\perp \to 0$; $H_{ci\perp} \to 0$ at $H_\parallel \to H_c$. In very thick samples ($\sqrt{\delta/d} \ll 1$) $B = H_c$ and Eq. (4) converts to Eq. (2) if $\rho_n^2(1-\rho_n)^2$ is replaced by $f_L(\rho_n)$; this explains correctness of the temperature dependence $\delta(T)$ in Refs. 11, 12.

For a perpendicular field ($H_\parallel = 0$) we have that (a) according to Eq. (8), B *decreases* with increasing H from H_c down to H_{ci}, in agreement with the μSR results [14]; and that (b) Eq. (7) reduces to Eq. (1), implying that the theoretical points in Fig. 2 are the same in our model. Hence our model, composed for the regular laminar structure, can be used for irregular laminar patterns as well.

Interestingly, we find that in a tilted field B is determined by $H_\perp$ (Eq. (8)). This implies that when $H_\perp$ is fixed and $H_\parallel$ is varied, ρ_n (the fraction D_n/D) in Eq. (6) varies in such a way that the total B remains constant.

In Fig. 3 the experimental data for $H_{ci\perp}$ at nonzero $H_\parallel$ are compared to the $H_{ci\perp}(H_\parallel)$ dependence given by Eq. (7). We find that Eq. (7) correctly describes the experimental data.

Fig. 4 presents the results for δ at $T = 1.7\,\mathrm{K}$ obtained in three ways. The circles represent δ calculated from Eq. (2) and Eq. (4) using our experimental data for average $D = 1/\aleph$ and $H_\perp$ at $\rho_n = 0.5$. A dashed line in Fig. 4 represents δ directly calculated using $\xi_0 = 380$ nm. We find that the results following from Eq. (4) agree with the directly calculated value of δ. However it is not the case for δ obtained using Eq. (2).

Fig. 5 presents experimental data for the average D obtained in two runs at T=1.7 K and $H_\parallel = 0.85H_c$ and corresponding theoretical expectations following from Eqs. (2) and (4). Solid circles are the data obtained at increasing $H_\perp$ with the sample cooled at $H_\perp = 0$. The data represented by open circles were taken after $H_\perp$ was

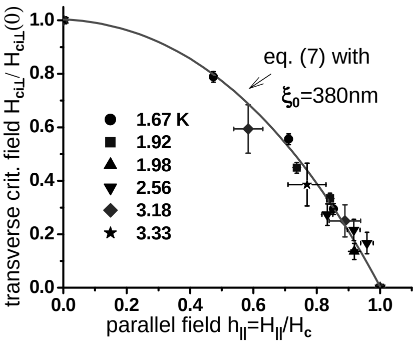

FIG. 3: The transverse critical field $H_{ci\perp}/H_{ci\perp}(0)$ versus $h_{\|} = H_{\|}/H_c$. $H_{ci\perp}(0)$ is $H_{ci\perp}$ at $H_{\|} = 0$.

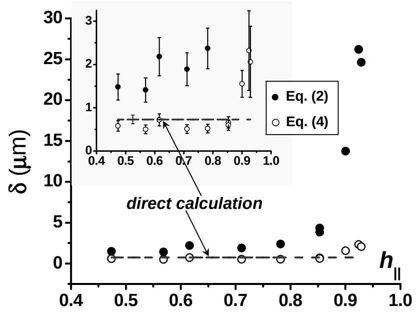

FIG. 4: The wall energy parameter δ inferred from MO images taken at $T = 1.7\,\mathrm{K}$ using Eq. (2) and Eq. (4) plotted on two scales. The dashed line represents the directly calculated $\delta = 1.4\xi_0/(1 - T/T_c)^{0.5}$, $T_c = 3.415\,\mathrm{K}$ and $\xi_0 = 380\,\mathrm{nm}$, with the error bar corresponding to the error of ξ_0 [10].

reduced from above $H_{ci\perp}$ down to $0.5H_{ci\perp}$. In Eq. (2) D is controlled by f_L; in our model the spacing function is $f = (1 - \rho_n^2)h_\perp^2$ with ρ_n and $h_\perp$ linked by Eq. (6). We find that both f_L and f are qualitatively consisted with the experimental data, however f_L "works" better at the high end of the IS, whereas f is better at the lower end. Therefore a refined model should also include contribution of the rounded corners.

Summarizing, performed magneto-optical study of the IS in the pure limit Pippard superconductor resulted in the development of a new theoretical model of the IS for a flat slab in an arbitrary oriented magnetic field. The model reproduces experimental data on the critical field H_{ci} for transverse and tilted field directions; the directly measured dependence $B(H_\perp)$ [14]; and the directly measured value of the Pippard coherence length [10]. The model allows one to infer δ from IS patterns in a strongly tilted field, where laminae are linear, and to make a plausible estimate of δ from H_{ci} at the transverse field, where laminae are corrugated. Overall, the model is a *good first order approximation* of the IS in a flat slab put forward by Landau more than 7 decades ago.

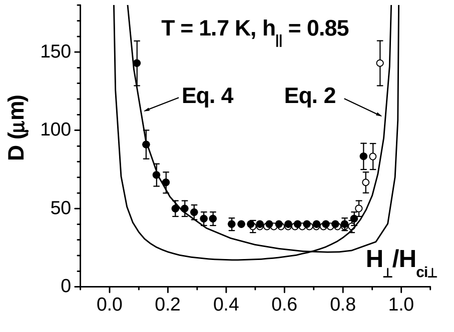

FIG. 5: Experimental data (circles) and theoretical curves for the period of the laminar flux structure.

A weak point of our model, which should be addressed in a refined approach, is an oversimplified form of L_{heal}. This is a major reason of discrepancy between experimental and theoretical $D(h_\perp)$ (Fig. 5), deviation of $\rho_n(h_\perp)$ in Eq.(6) from a linear dependence following from linearity of $R(H_\perp)$, and deviation of $\delta(h_\|)$ from a constant value at large $h_\|$ (Fig. 4). To resolve this issue measurements of the magnetic field near the surface outside and inside the sample are desirable. We note that this is also relevant for elucidation of the vortex core structure in type-II superconductors [18].

This work was supported by NSF (DMR 0904157) and by the Science Foundation - Flanders (FWO, Belgium).

[1] G. R. Berdiyorov, A. D. Hernandez-Nieves, M. V. Milosevic, F. M. Peeters, and D. Domnguez, Phys. Rev. B **85**, 092502 (2012).

[2] R. Prozorov, Phys. Rev. Lett. **98**, 257001 (2007).

[3] J. E. Sonier, Rep. Prog. Phys. **70**, 1717 (2007).

[4] A. A. Abrikosov, *Fundamentals of the theory of metals* (Elsevier Science Pub. Co., 1988)

[5] L. D. Landau, ZhETF **7**, 371 (1937).

[6] M. Tinkham, *Introduction to Superconductivity* (McGraw-Hill, 1996).

[7] L. D. Landau and E.M. Lifshitz, 1984).

[8] P. G. De Gennes, *Superconductivity of Metals and Alloys* (Perseus Book Publishing, L.L.C., 1966).

[9] R. P. Huebener *Magnetic flux structures in superconductors*, 2nd ed. (Springer-Verlag, 2001).

[10] V. Kozhevnikov, A. Suter, H. Fritzsche, V. Gladilin, A. Volodin, J. Cuppens, T. Prokscha, E. Morenzoni, M. Van Bael, K. Temst, C. Van Haesendonck, J. Indekeu, cond-mat. 1209-3502 (2012).

[11] Yu. V. Sharvin, ZhETF **38**, 298 (1960).

[12] Yu. V. Sharvin, ZhETF **33**, 1341 (1957).

[13] L. D. Landau, ZhETF **13**, 377 (1943).

[14] V. S. Egorov, G. Solt, C. Baines, D. Herlach, and U. Zimmermann, Phis. Rev. B **64**, 024524 (2001).

[15] I. T. Faber, Proc. Roy. Soc. A **248**, 460 (1958).

[16] I. E. Dzyaloshinskii, Dokl. Akad. Nauk SSSR **105**, 244 (1955).

[17] D. K. Finnemore, and D. E. Mapother, *Phys. Rev.* **140**, A507 (1965).

[18] E. H. Brandt, Phys. Rev. B **71**, 014521 (2005).